Caraka Tani
Journal of Sustainable Agriculture
ISSN 2613-9456 (Print) 2599-2570 (Online)

Caraka Tani: Journal of Sustainable Agriculture, 40(2), 209-230, 2025
URL: https://jurnal.uns.ac.id/carakatani/article/view/93122
DOI: http://dx.doi.org/10.20961/carakatani.v40i2.93122

Assessing Land Use Intensity and Ecosystem Service Dynamics in Citarum Watershed, Indonesia

Irmadi Nahib[1,2], Widiatmaka[3*], Suria Darma Tarigan[3], Wiwin Ambarwulan[2] and Fadhlullah Ramadhani[4]

[1]Natural Resources and Environmental Management Science (NREMS) Study Program, Graduate School of IPB University, Bogor, Indonesia; [2]Research Center for Limnology and Water Resources, National Research and Innovation Agency of Indonesia (BRIN), Cibinong, Indonesia; [3]Department of Soil Science and Land Resource, Faculty of Agriculture, IPB University, Bogor, Indonesia; [4]Research Center for Geoinformatics, National Research and Innovation Agency of Indonesia (BRIN), Bandung, Indonesia

[*]*Corresponding author:* widiatmaka@apps.ipb.ac.id

Abstract

Changes in land use and land cover (LULC) significantly impact ecosystem services (ES), often leading to land degradation and disrupting natural balance. This study examines how LULC changes have influenced total ecosystem services (TES) in Citarum Watershed over the past decade. Specifically, researchers analyze (1) the shifts in LULC and key ES components—water yield (WY), soil conservation (SC), and carbon storage (CS)—from 2010 to 2020, (2) the spatial relationship between land use intensity (LUI) and ES, and (3) the synchronization and distribution patterns of LUI and TES using a coupling coordination degree (CCD) model. The findings reveal significant LULC changes between 2010 and 2020, with bare/shrubland and agricultural areas expanding by 88.37% and 2.25%, while forest land and lakes declined by 0.78% and 0.09%. These transformations affected ES values, as WY and CS decreased by 15.01% and 4.98%, whereas SC increased by 12.03%. Overall, TES declined by 7.54%, with the steepest reduction (17.70%) observed in the downstream region. The coupling coordination analysis highlights an imbalance between LUI and TES, with 65 to 68% of sub-districts classified as imbalanced. These results underscore the urgent need for integrated land-use planning strategies to restore ecosystem balance and promote sustainability in Citarum Watershed.

Keywords: conservation; ecology; environmental protection; natural resources; sustainability

Cite this as: Nahib, I., Widiatmaka, Tarigan, S. D., Ambarwulan, W., & Ramadhani, F. (2025). Assessing Land Use Intensity and Ecosystem Service Dynamics in Citarum Watershed, Indonesia. *Caraka Tani: Journal of Sustainable Agriculture*, *40*(2), 209-230. doi: http://dx.doi.org/10.20961/carakatani.v40i2.93122

INTRODUCTION

Ecosystem services (ES) refer to the inherent services provided by the environment that directly or indirectly enhance the long-term welfare of human beings. These services are classified into four categories (Millennium Ecosystem Assessment, 2005): provisioning, regulating, supporting, and cultural. Humans can obtain both direct and indirect benefits from the processes that take place in the ecosystems (Costanza et al., 1998). Ecosystems are very important in economic development and human welfare; therefore, ecosystem changes need to be directed to provide benefits for humans. Wrong direction in ecosystem modifications might result in the deterioration of environmental sustainability and a rise in expected hazards (Duraiappah, 2011).

Unregulated economic development activities are gradually deteriorating the functioning of global and regional ecosystems (Strassburg et al., 2020). The Millennium Ecosystem Assessment (MEA) Report (2005) concludes that 15 out of 24 ES have seen adverse effects globally in the

* *Received for publication September 16, 2024*
Accepted after corrections February 10, 2025

last 50 years. Human-induced changes in land use and land cover (LULC) are responsible for 60% of the decrease in ES provision (Jew et al., 2019). ES value has become important in tackling significant issues associated with ES (De Groot et al., 2012). Evaluating the impact of land use intensity (LUI) on ES and functions is crucial because of the potential for LUI to modify essential elements of ecosystem function, such as conflicts between ecosystem functions and services and their benefits (Felipe-Lucia et al., 2020). Examining the correlation between LUI and ES is crucial for improving human welfare and establishing theoretical principles for strategic decision-making in regional development regarding land use and ES.

Strategic regional development planning should take into account the changing environmental conditions caused by changes in LULC (Gomes et al., 2021b). Changes in LULC can result in land degradation, which hinders the availability of ES in certain regions and destabilizes the establishment of sustainable ecosystems (Bryan et al., 2018). LULC refers to alterations in the categories of land use and modifications in the intensity and spatial configurations of land (Fu et al., 2015).

In more detail, the subsequent impact of land use change is a change in the function of ES. Suwardi et al. (2023) conducted a review study investigating N_2O emissions across different agricultural systems, including maize, peanut, and cassava fields on mineral soils in Bogor Regency, West Java, as well as Acacia plantations and primary forests in tropical peatlands in Bengkalis Regency, Riau. The study analyzed the effects of land use, fertilization practices, and rainfall patterns. The results indicated that N_2O emissions were primarily influenced by land use type, fertilizer application, and soil disturbance. These findings emphasize the need for effective fertilizer management and soil conservation (SC) strategies. Moreover, the significantly higher N_2O emissions in peatlands compared to mineral soils highlight the critical need for targeted mitigation efforts in these ecosystems.

While the relationship between changes in LUI and ES has been somewhat disregarded (Zheng et al., 2022), fluctuations in LUI also affect ES and their related functions (Wen et al., 2019). The study conducted by Xu et al. (2016) used variance analysis and correlation methods to investigate the impact of LUI on ES and human well-being. The study's findings indicated that increased levels of LUI facilitate food production, SC, and climate control. Felipe-Lucia et al. (2020) suggest that the expression of ES and its functions can rise at moderate levels of LUI. Still, the extent of this positive relationship decreases at greater LUI levels.

A crucial aspect of regional development planning, particularly in watershed management, that has received limited attention in previous research is the integration of LUI and ES into watershed planning. Previous studies have often overlooked the importance of incorporating diverse decision-making preferences into regional planning and the identification of conservation areas (Li et al., 2023). The uncoordinated development of LULC changes and ES in the Citarum Watershed poses a significant threat to the ecological environment, necessitating a thorough evaluation of ES by examining the correlation between LUI and ES (Agaton et al., 2016; Siswanto and Francés, 2019). Research on the relationship between LUI and ES in Indonesia remains insufficient, underscoring the need for further exploration.

The Citarum Watershed is one of the critical watersheds prioritized for intervention. Research on ES has been conducted extensively in this watershed. For instance, Pranoto et al. (2024) highlighted the Citarum Watershed's critical role in providing ES, particularly as a regional water supplier and a source for hydropower generation. Conversely, several research focused mainly on individual services, such as water yield (WY) (Nahib et al., 2022) and SC (Nahib et al., 2024b).

Understanding the relationships between ESs is vital for sustainable watershed management (Nahib et al., 2024b). The 2010 to 2020 data play a critical role in assessing the West Java Province Long-Term Development Plan (RPJP) for the 2000 to 2020 period (Development Planning Agency at Sub-National Level of West Java Province, 2008). The evaluation was divided into two phases: the 2000 to 2010 and the 2010 to 2020 period, representing the second 10-year assessment. This analysis seeks to identify trends observed over the past two decades and forecast potential changes for the next 20 years, with a focus on risks, impacts, and trends associated with anticipated environmental dynamics (Malinga et al., 2015).

The present work aims to fill this research gap by utilizing a coupling coordination degree (CCD) model to examine the patterns and variations in LUI and total ecosystem services (TES) in the Citarum Watershed. The objectives of this study are: (1) to examine LULC changes and ES, WY, SC, and carbon storage (CS) between 2010 and 2020; (2) to investigate the bivariate spatial autocorrelation between LUI and ES during the same period and location; and (3) to explore the synchronization behaviors and spatiotemporal distribution of LUI and TES in the watershed using a CCD model. The results are expected to be useful for regional planners and decision-makers for sustainable watershed management.

MATERIALS AND METHOD

Study area

The study was carried out in the Citarum Watershed, covering an area of 690,916 ha in the West Java Province, Indonesia (Figure 1). Geographically, the research location is situated within the longitudes of 106°51’ and 107°51’ E and the latitudes of 7°19’ and 6°24’ S. The research location is in a tropical climate area with a yearly average rainfall of 2,358 mm. The Citarum River is crucial for power generation, agricultural activities, and the provision of freshwater to inhabitants in many regencies of West Java. The river traverses the watershed and it is controlled by three prominent dams, namely Saguling, Cirata, and Jatiluhur.

The topography in this region exhibits considerable variation, including prominent hills and volcanic structures. The slopes range from 5 to 90%. The upstream mountains have elevations ranging from 750 to 2,300 meters above sea level (m asl), whereas the plains have comparatively moderate volcanic terrain characteristics (Minister of Public Works and Housing Regulation, 2016; Sholeh et al., 2018).

The Citarum Watershed can be classified as upstream, midstream, and downstream watersheds based on landform or morphological features. The topography in the upstream areas is similar to that of the Bandung Basin, a sizable basin between 625 and 2,600 m asl. Tuff, lava, breccia, and lapilli comprise most of the geological composition of the upper Citarum areas. In the highland and mountainous regions, the minimum temperature is 15.3 °C, with an average of 4,000 mm of rainfall annually (Minister of Public Works and Housing Regulation, 2016; Sholeh et al., 2018). According to Khairunnisa et al. (2020), the soil types found in the upper Citarum Watershed are Latosol (35.7%), Andosol (30.76%), Alluvial (24.75%), Red-Yellow Podzolic (7.72%), and Regosol (0.86%).

Data used

This study utilizes ES data, including WY, SC, and CS, as presented in Appendix 1. The ES of Citarum Watershed has been studied by Nahib et al. (2022; 2024b), and the ES output (WY, CS, and SC) was used in this research. The TES value was calculated by using the three ES matrices. Additionally, the LUI value was determined by multiplying the factor score for each LULC type by its respective area.

Data analysis

Four steps were carried out to investigate the CCD relationship between LULC and TES (Figure 2). In the first step, an analysis of the changes in the degree of LULC dynamics and LUI was carried out using LULC data from 2010

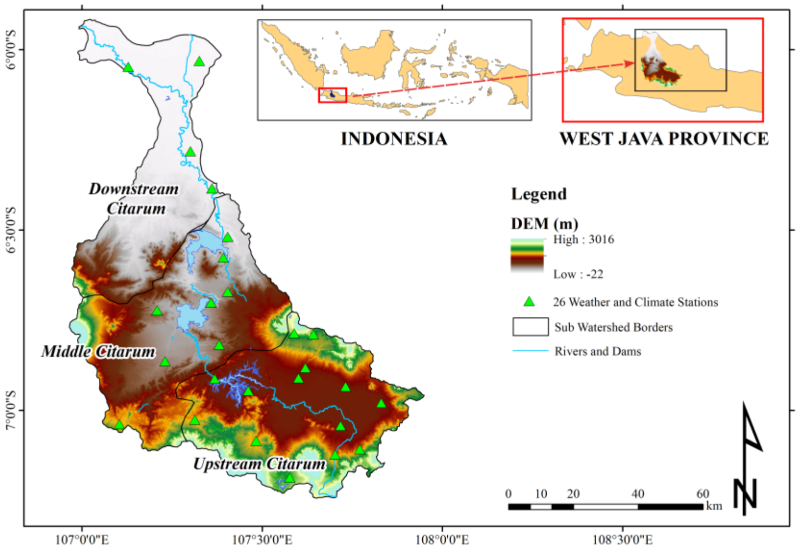

Figure 1. Research location of the Citarum Watershed, West Java Province, Indonesia

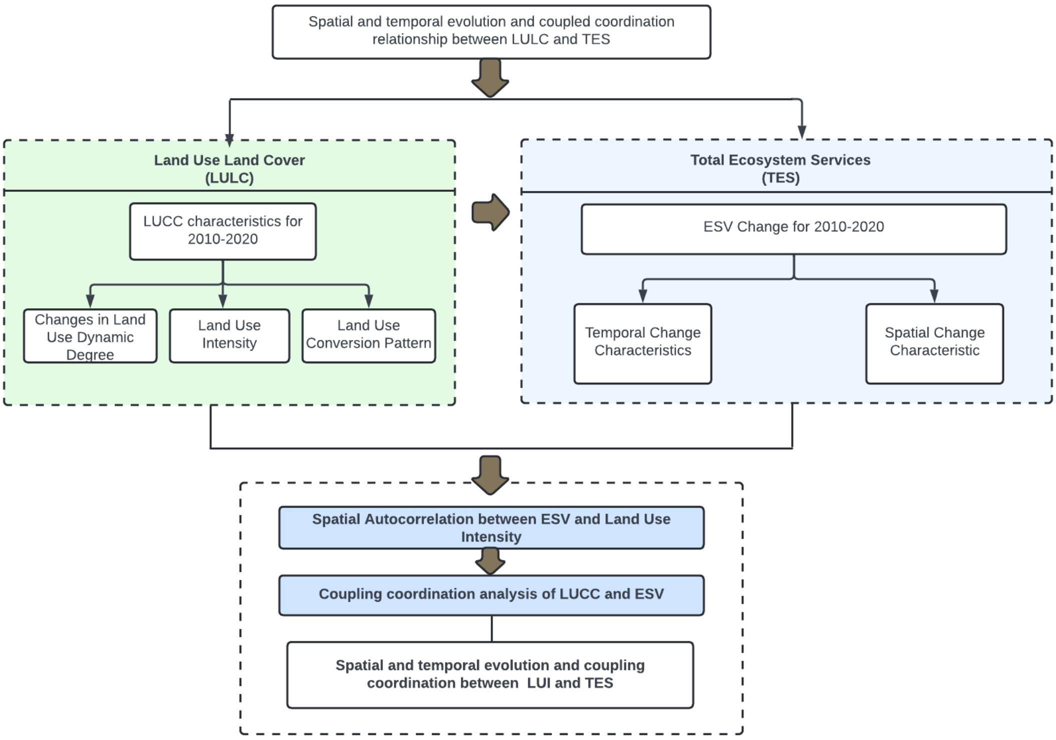

Figure 2. Research framework

and 2020. This analysis used LUI techniques, a conversion matrix, and land use dynamics at a resolution of 30 m. In the second step, three primary variables of ES (CS, SC, and WY) were used to determine the TES. Temporal and spatial change analyses were conducted using TES data from 2010 and 2020.

In the third step, the sub-district boundaries were established, and TES and LULC were calculated for each sub-district using the zonal statistical tools on the ArcGIS 10.8 platform, as presented in Appendix 2. In the fourth step, the relationship between LULC and TES was investigated, as well as CCD analysis and local spatial autocorrelation were used.

LULC dynamic

The Google Earth Engine (GEE) platform was employed to produce satellite images free of cloud interference. The Landsat datasets, which featured atmospherically corrected surface reflectance, were processed using the Landsat Ecosystem Disturbance Adaptive Processing System (LEDAPS) algorithm (Yulianto et al., 2021). Landsat pixels were classified into six LULC categories through a supervised classification method utilizing the Random Forest (RF) algorithm on the GEE platform.

To make clear the transitions between various land use categories within the study area, the properties of LULC were studied using a land use-type transfer matrix. Equation 1 represents this matrix.

$$Y_{ij} = \begin{bmatrix} Y_{11} & Y_{12} & \dots & Y_{1n} \\ Y_{21} & Y_{22} & \dots & Y_{2n} \\ Y_{n1} & Y_{n2} & \dots & Y_{nn} \end{bmatrix} \quad (1)$$

Where Y_{ij} represents the amount (hectares) of LULC that changed from category i (e.g., forest, agriculture, built-up, water, etc.) at time t_1 (beginning) to category j (e.g., forest, agriculture, built-up, water, etc.) at time t_2 (end).

Both single and integrated dynamic land use models were created to enhance the portrayal of conversion intensity and land use coverage. Equation 2 defines the single land use dynamics model.

$$D = \frac{L_2 - L_1}{L} \text{ x } \frac{1}{T} 100\ \% \quad (2)$$

Where the degree of single land use dynamics is denoted by D, the study period is T, the area of a certain land use type at the beginning is represented by L_1, the area of that land use type at completion is represented by L_2, and so on.

For LUI, the classification is divided into four classes: Class 1 (unutilized land and bare land), Class 2 (water bodies, lakes, virgin forests, plantation forests, shrubs, and grasslands), Class 3 (agricultural land, including paddy fields, estate crop plantations, and dry farming), and Class 4 (construction land, including settlement areas and airports). This classification is defined by Equation 3.

$$Q_a = 100 \times \sum_{i=1}^{n} A_i \times C_i \quad (3)$$

Where Q_a is combined LUI, A_i denotes the level of LUI, and C_i represents the corresponding class.

TES

This study looks at three ES: WY, SC, and CS. The previous research has provided the measurements for these ES in the research area (Nahib et al., 2022; Nahib et al., 2024b).

The WY module within the lnVEST model is used to analyze the spatial distribution of WY within the designated study area. Operating on the principle of water balance, the module defines WY as the residual water post-precipitation within each grid, accounting for plant transpiration and surface evaporation. It assumes that the WY of each grid unit eventually reaches the watershed outlet via surface and subsurface runoff. Estimation of WY involves factors such as precipitation, potential evapotranspiration, root system characteristics, and soil depth. This estimation is further refined by incorporating runoff data from hydrological stations located at the basin's outlet. Ultimately, the model calculates the WY for each grid within the basin, employing specific algorithms outlined by Equation 4 and 5 (Sharp et al., 2020).

$$Y_{xj} = \left(1 - \frac{AET_{xj}}{P_x}\right) \times P_x \quad (4)$$

$$\frac{AET(x)}{P(x)} = \frac{1 + w_x R_{xj}}{1 + w_x R_{xj} + 1/R_{xj}} \quad (5)$$

Where Y_{xj} represents the WY of the x-th grid of land use type j (m^3 hm^{-2}), AET_{xj} represents the annual actual evapotranspiration of the x_{-th} grid of land use type j (mm), P_x represents the annual average precipitation of the x-th grid (mm), R_{xj} represents the dryness index of the x-th grid of land use type j, and W_x represents the available water content of vegetation.

The sediment delivery ratio (SDR) module within the InVEST model assesses SC within the specified study region. Following the potential soil loss equation, SC is determined by deducting potential soil erosion (RKLS) from actual soil erosion (USLE) to estimate soil loss per pixel. This calculation is expressed by Equation 6, 7, and 8 (Sharp et al., 2020).

$$SC_i = RKLS_i - USLE_i \quad (6)$$

$$RKLS_i = R_i \times K_i \times LS_i \quad (7)$$

$$USLE_i = R_i \times K_i \times LS_i \times C_i \times P_i \quad (8)$$

Where SC_i is SC, $RKLS_i$ is the potential erosion amount, $USLE_i$ is the actual erosion amount, R_i is rainfall erosivity factor, K_i is soil erodibility factor, LS_i is the slope length factor, C_i is the vegetation cover management factor, and P_i is the factor of water and SC measures.

The carbon module within the InVEST model is employed to quantify CS within the designated study area. CS within the present landscape is assessed by considering land use type data across various periods and the corresponding carbon pool storage. The calculation is conducted by Equation 9 (Sun et al., 2018; Sharp et al., 2020).

$$CS_{total} = CS_{above} + CS_{below} + CS_{soil} + CS_{dead} \quad (9)$$

The total CS (CS_{total}) is comprised of various components: aboveground carbon storage (CS_{above}), underground carbon storage (CS_{below}), soil carbon storage (CS_{soil}), and carbon storage of dead organic matter (CS_{dead}). All values are expressed in units of mg ha^{-2}.

Three inputs were used to determine TES, such as WY, SC, and CS. The values of these ES were standardized to a range of 0 to 1, as their units varied. The process outlined in Equation 10 (Peng et al., 2017) is then applied to get TES by averaging the standardized values of each ES.

$$ES_i = \frac{ES_{i,obs} - ES_{i,min}}{ES_{i,max} - ES_{i,min}} \quad (10)$$

Where ES_i represents the standard value of type *i* ES, $ES_{i,obs}$ denotes the raw value of *i* ES, and $ES_{i,min}$ and $ES_{i,max}$ represent the minimum and maximum values of *i* ES, respectively.

Spatial autocorrelation test

Examining spatial autocorrelation enables the identification of geographical grouping and heterogeneity in attribute values. Typically, this analysis is assessed using global and local Moran's I indices, which provide insights into the spatial distribution features (Anselin, 1995). Some researchers studied the geographical aggregation and dispersion patterns between ES and LUI using Bivariate Moran's I, which is a statistical measure that incorporates both global and local indicators of bivariate spatial autocorrelation (Anselin, 1988; Xiao et al., 2020). The present study employed bivariate spatial autocorrelation analysis to investigate the geographical relationship between ES and LUI.

This study utilized the global Moran's I index, which takes values from -1 to 1. A negative Moran's I value denotes an inverse relationship between LUI and ES, whereas a positive Moran's I value suggests a direct positive relationship between the two variables. The proximity of Moran's I index to zero indicates that the association between ES and LUI adheres to a random or scattered pattern.

CCD between LUI and TES

A physics notion inspired the interwoven interactions between TES and LUI (Kurniawan et al., 2019; Zhu et al., 2022). This concept highlights that when two or more systems interact, they can mutually benefit from a positive dynamic relationship (Dong and Li, 2021). Researchers created a model to determine the coupling between LUI and TES using this physics theory of coupling, as shown by Equation 11.

$$C = 2\sqrt{\frac{(LUI_x \times TES_x)}{(LUI_x + TES_x)^2}} \quad (11)$$

Where, *C* represents the coupling strength between *LUI* and *TES*, which goes from 0 to 1. *LUI* represents the evaluation value for LUI, and *TES* shows the comprehensive assessment for total ES. Higher values of *C* indicate greater *LUI* and *TES* interactions.

It is essential to understand, nevertheless, that the coupling degree does not represent the developmental state of the two systems; rather, it only indicates the degree of correlation between them. Both systems could have low values and high coupling degrees at the same time. Therefore, it is critical to understand the difference between horizontal solid coupling and high coupling values. Equation 12 and 13 of the CCD model were used to measure the degree of coordination between LUI and ES.

$$D = \sqrt{C \times T} \quad (12)$$

$$T = \alpha LUI_x + \beta TES_x \quad (13)$$

Where *D* stands for the *LUI* and *TES* coordination coefficient. *T* is the overall synergy effect as represented by the two systems' thorough assessment index. α and β denote the weight coefficients assigned to the two systems, typically ranging between 0 and 1. For this study, it is assumed that urbanization and the ecosystem hold equal significance. Hence, both α and β were assigned the same value of 0.5 (Zhang and Li, 2020). The CCD has been categorized by recent studies into five levels of imbalance and coordination: necessary coordination (0.4 ≤ CCD < 0.6), decent coordination (0.6 ≤ CCD < 0.8), strong coordination (0.8 ≤ CCD ≤ 1), severe imbalance (0 ≤ CCD < 0.2), and moderate imbalance (0.2 ≤ CCD < 0.4) (Zhang et al., 2022).

RESULTS AND DISCUSSION

LULC dynamic

Image classification is prone to various errors, making accuracy assessment essential. The analysis shows that the 2010 Landsat image achieved a Kappa coefficient of 84% and an overall accuracy of 88%. Likewise, the 2020 Landsat image recorded a Kappa coefficient of 82% and an overall accuracy of 83%. These results confirm that both the Kappa and overall accuracy values exceed the 80% threshold, indicating they fall within an acceptable range. Additionally, all LULC categories have Kappa values above 80%, reinforcing their reliability as indicators of accuracy (Shao et al., 2019; Islami et al., 2022).

By analyzing Landsat images from 2010 and 2020, the LULC types are presented in Table 1 and Figure 3. Table 1 presents the examination

Table 1. The area of each class, change, and degree of LULC of Citarum Watershed (2010 to 2020)

LULC	2010		2020		Change 2010–2020		Degree LULC
	ha	%	ha	%	ha	%	
Forest	101,712.40	14.82	100,793.86	14.82	918.54	(0.78)	(0.08)
Construction land	72,482.33	11.39	77,984.19	11.47	502.18	0.65	0.06
Bare/shrubland	12,838.69	1.89	26,486.88	3.90	(13,648.19)	88.37	8.83
Agricultural land	439,801.45	64.68	452,618.96	66.55	12,817.51	2.91	0.29
Fishpond	19,719.26	2.90	20,146.55	2.96	427.29	2.17	0.22
Lake	15,221.70	2.24	15,208.41	2.24	(13.29)	(0.09)	(0.01)

Note: () = Indicates a minus (decrease)

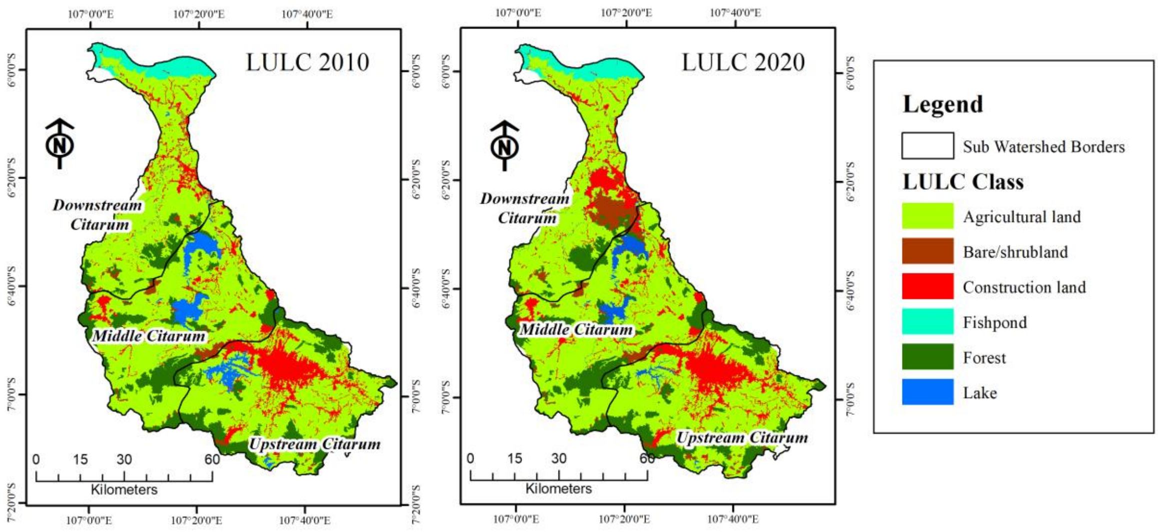

Figure 3. LULC in Citarum Watershed (a) Year 2010, (b) Year 2020

of LULC variations throughout the 10 years (2010–2020). Furthermore, the degree of LULC is shown in Table 1 and was computed using Equation 2.

Table 1 illustrates that the dominant LULC types in 2010 were agricultural land (64.68%), forest (14.82%), construction land (11.39%), and bare/shrubland (3.90%). The LULC in 2020 was relatively the same as the LULC in 2010. Significant increases were observed in the LULC types of bare/shrubland (88.37%) and agricultural land (2.91%). Conversely, there were decreases in forest cover (2.91%) and lake area (0.09%). Overall, LULC conditions did not undergo substantial changes during this period, as depicted in Figure 4, with detailed changes presented in the LULC change matrix in Table 2.

According to Equation 2, in the 2010 to 2020 period, the level of LULC dynamics integration changed by 0.258%. The integrated dynamic degree for 2010 to 2020 is 0.816%. The analysis reveals a fluctuating trend in integrated dynamics across different land use types, with an initial increase. These statistics were used to rank each LULC type's dynamic degree from highest to lowest as follows: bare land/shrub > agricultural land > fishpond > forest > lake. Between 2010 and 2020, changes in LULC in Citarum Watershed have been largely impacted by anthropogenic activities, especially urbanization (increased construction land) and deforestation (Nahib et al., 2023). The decrease in forests and the increase in construction areas indicate heightened anthropogenic activities, particularly urbanization and deforestation (Nahib et al., 2024b).

In the upper Citarum Watershed, Siswanto and Francés (2019) reported a 141% growth in urban areas, resulting in a decrease in rice fields and the replacement of forests with cultivated lands. These alterations have significantly impacted the region's hydrological and sedimentological processes, leading to a decrease in evapotranspiration, an increase in water output, and an increase in erosion-prone areas. Furthermore, because of changes in LULC

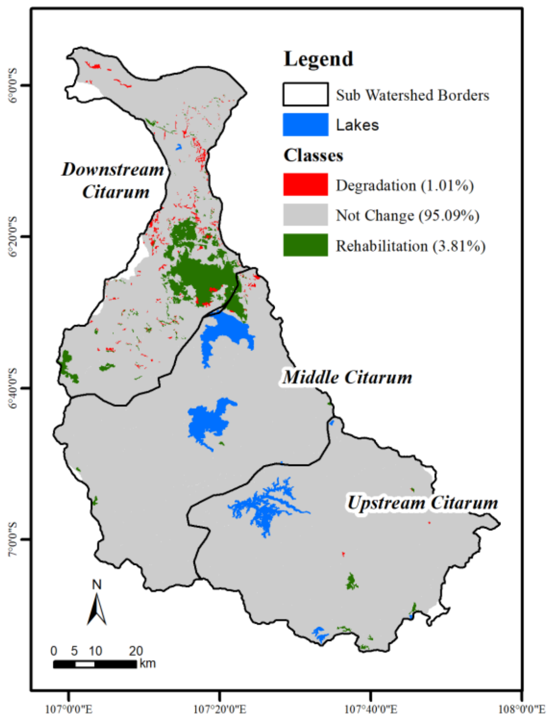

Figure 4. LULC changes in Citarum Watershed from 2010 to 2020

Table 2. LULC change matrix, 2010 to 2020 (ha)

2010	2020						
Type of LULC	Forest	Bare/shrubland	Construction land	Agricultural land	Lake	Fishpond	Total
Forest	97,842.36	1,290.29	18.87	2,422.71			101,712.40
Bare/shrubland	483.49	12,294.41	37.62	12,730.22			12,838.69
Construction land	45.31	171.96	68,646.60	3,618.47			72,482.33
Agricultural land	2,422.71	12,730.22	9,281.10	433,184.94		427.28	439,801.44
Lake		13.28			15,208.41		15,221.70
Fishpond						19,719.26	19,719.26
Total	100,793.87	26,486.88	77,984.19	452,618.96	15,208.41	20,146.55	

patterns and rapid urban growth, the expansion of urban areas is predicted to worsen the urban heat island (UHI) effect, raising temperatures (Derdouri et al., 2021).

Yusuf et al. (2018) found several variables affecting LULC shifts in Citarum Watershed between 2010 and 2020, including (1) economic activity and shifts in the economy that lead to modifications in land use (the extension of agricultural land for commercial usage); (2) population growth and social dynamics, which increase demand for land and result in LULC changes; and (3) natural events such as floods, which can alter land use patterns as affected areas may be converted into agricultural land or other uses to mitigate future impacts.

Key drivers of LULC changes in Citarum Watershed have been studied by Nahib et al. (2023) and the results show that rapid urbanization, forest conversion, and agricultural expansion are the main factors influencing LULC. Meanwhile, Syaban and Appiah-Opoku (2024) also studied LULC changes. They concluded that natural habitats and agricultural lands were converted into urban areas due to urbanization. In contrast, habitat degradation, decreased biodiversity, and conversion of natural habitats into agricultural lands were caused by forest conversion and agricultural growth. According to Wang et al. (2020), these elements work together to cause major LULC changes in Citarum Watershed, which lead to environmental problems such as soil erosion and decreased WY. Land conversion for agricultural and urban areas has resulted in changes in the topography, which affects the watershed’s ecosystems and water resources. According to previous research (Husodo et al., 2021), land shrinkage frequently happens in places bordering Bandung, most likely due to the city’s growth into neighboring areas. The study reveals that sub-districts experiencing the largest shrinkage are those with relatively small areas, such as Cipatat (74%) and Batujajar (83%) (Agaton et al., 2019). However, between 1989 and 2019, some sub-districts, such as Bojongsoang, Slawi, and Tanjungsari, increased in vegetated land area (Husodo et al., 2021).

ES dynamic

Figure 5 and Table 3 illustrate the spatial distribution and changes of three ESs within the Citarum Watershed over a decade, from 2010 to 2020. These visual tools offer valuable insights into the evolving dynamics and spatial patterns of ESs in the study area.

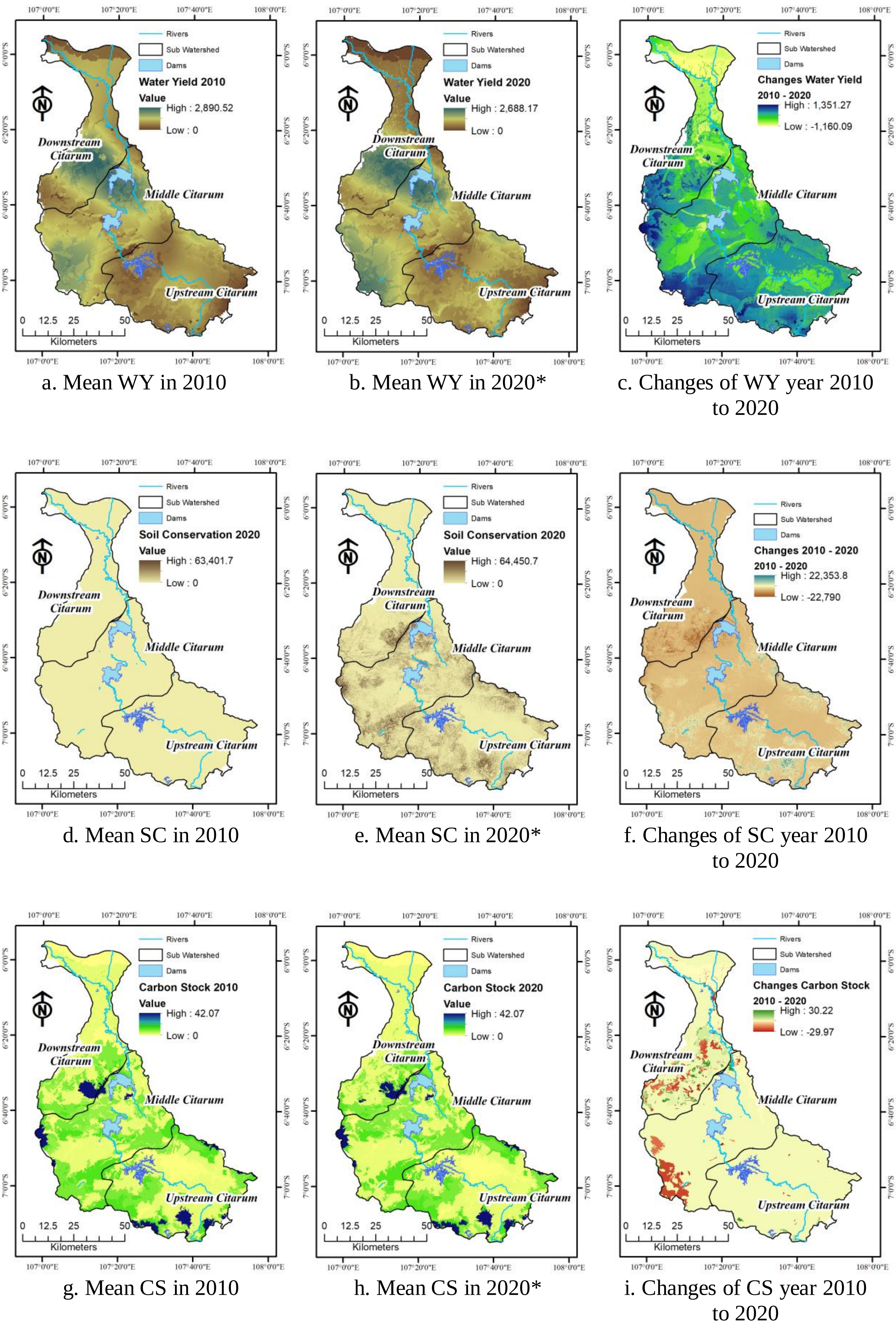

a. Mean WY in 2010
b. Mean WY in 2020*
c. Changes of WY year 2010 to 2020
d. Mean SC in 2010
e. Mean SC in 2020*
f. Changes of SC year 2010 to 2020
g. Mean CS in 2010
h. Mean CS in 2020*
i. Changes of CS year 2010 to 2020

Figure 5. The grid-scale spatial distribution of ESs
Note: *Source = Nahib et al. (2024b)

Table 3. The total amount of ESs in Citarum Watershed (2010 to 2020) and its changes

Name subwatershed	WY 2010 Mean (10^3 m^3 ha^{-1})	WY 2010 Total (10^8 m^3)	WY 2020 Mean (10^3 m^3 ha^{-1})	WY 2020 Total (10^8 m^3)	Changes 2010–2020 Mean (10^3 m^3 ha^{-1})	Changes 2010–2020 Total (10^8 m^3)
Upstream	10.02	24.09	9.01	21.74	-1.01	-2.35
Middle	16.13	39.93	14.25	35.36	-1.88	-4.57
Downstream	15.07	27.68	11.36	20.83	-3.71	-6.85
Total	13.74	91.70	11.54	77.93	-2.20	-13.77

Name subwatershed	SC 2010 Mean (tons 10^3 ha^{-1})	SC 2010 Total (10^8 tons)	SC 2020 Mean (tons 10^3 ha^{-1})	SC 2020 Total (10^8 tons)	Changes 2010–2020 Mean (tons 10^3 ha^{-1})	Changes 2010–2020 Total (10^8 tons)
Upstream	3.74	9.09	4.89	11.89	1.15	2.80
Middle	5.61	14.04	6.11	15.29	0.50	1.25
Downstream	2.50	4.56	2.10	3.84	(0.40)	-0.72
Total	3.95	27.69	4.49	31.02	0.54	3.33

Name subwatershed	CS 2010 Mean (tons 10^3 ha^{-1})	CS 2010 Total (10^8 tons)	CS 2020 Mean (tons 10^3 ha^{-1})	CS 2020 Total (10^8 tons)	Changes 2010–2020 Mean (tons 10^3 ha^{-1})	Changes 2010–2020 Total (10^8 tons)
Upstream	51.55	12.54	51.79	12.60	0.24	0.06
Middle	53.68	13.46	49.47	12.40	(4.21)	-1.06
Downstream	39.24	7.31	35.69	6.65	(3.55)	-0.66
Total	4.82	33.31	4.58	31.65	(0.24)	-1.66

Sources: Nahib et al. (2024b)

Table 3 indicates an overall decline in WY and CS within the Citarum Watershed from 2010 to 2020, while SC showed an increase during the same period. In 2010 and 2020, the WYs were recorded at 91.70×10^8 m^3 and 77.93×10^8 m^3, respectively, indicating a decline. The total WY in 2020 decreased by 13.8×10^8 m^3 (15.00%) compared to 2010. Notable spatial variation in WY was observed in 2020, with the midstream area having the highest unit WY, followed by the downstream area, while the upstream area recorded the lowest value. A decline in WY was observed across all subwatersheds from 2010 to 2020. The reduction was generally modest, except for the downstream area, which experienced a more pronounced decrease of 9.74% in the upstream, 11.44% in the midstream, and 24.75% in the downstream regions.

The trend of SC in Citarum Watershed is rising. In 2010, the total SC was 27.68×10^8 tons, increasing to 31.05×10^8 tons in 2020. Over 10 years, SC increased by 3.33×10^8 tons (12.05%). The improvement of SC in the Citarum Watershed reflects increasing efforts to protect and preserve soil in the area. This can be achieved through practices such as contour farming, terracing, and the use of organic materials to enhance soil structure and reduce erosion.

Table 3 indicates a declining trend in the CS of Citarum Watershed, with values of 31.31×10^8 and 31.65×10^8 tons in 2010 and 2020, respectively. However, the overall rate of decrease was rather gradual. In 10 years (2010 to 2020), there was a decrease in CS of 1.66×10^8 tons (4.98%).

The conversion of forested areas into non-forest uses not only affects CS but also compromises other ES such as water regulation and SC. Forests play a critical role in maintaining water quality and availability; their degradation can lead to increased sedimentation and flooding (Pitaloka et al., 2020; Nahib et al., 2024a). Citarum Watershed has undergone extensive urbanization and agricultural expansion, leading to the transformation of forested and agricultural areas into built-up zones. This land use shift has been associated with a notable decline in aboveground CS. For instance, a study in Rancakalong Sub-district recorded a reduction of 11,096 tons in aboveground CS from 2009 to 2021, primarily driven by the loss of mixed gardens (Malik et al., 2023).

TES and changes

Equation 10 was implemented for calculating TES values, as shown in Figure 6 and Table 4. Figure 6 represents the spatial distribution and variation of TES in Citarum Watershed: Figure 6a displays TES conditions in 2010, Figure 6b represents TES conditions in 2020, and Figure 6c illustrates the changes in TES between 2010 and 2020, both exhibit relatively similar distribution patterns. Low TES values were generally found in the central and western parts of the watershed. High TES values were typically found in the southern (upstream) and northern (downstream). Changes in TES from 2010 to 2020 are presented in Figure 6c, which shows that, overall, the changes were relatively small, with larger changes occurring only in the western part of the watershed.

Referring to Table 4, in the 2010 to 2020 period, the TES of Citarum Watershed decreased (7.54%). The largest decrease in TES occurred in the downstream Citarum Watershed area (17.70%). Meanwhile, the upstream Citarum Watershed area has a constant TES value, only a decrease of 0.88%. Land use changes are influenced by natural and socio-economic causes, which result in regional differences in ES. Previous research has shown that urban expansion into ecological areas, such as farmland, woodlands, and water bodies, can result in a decline in ES (Maimaiti et al., 2022). Regional variations in the spatial distribution of ES are also influenced by natural topography (Liu et al., 2019).

Throughout the study period, the decline in ES paralleled the increase in built-up land. The study area's fall in ES was mostly caused by urban expansion, which grew at the fastest pace and reduced ecological lands like forests. The findings from a previous study by Nahib et al. (2024), which utilized the Multiscale Geographically Weighted Regression (MGWR) Model approach, revealed that the coefficients for topography, climate, vegetation, and socio-economic factors varied spatiotemporally in their impact on the trade-off synergy among ESs. Vegetation contributed the most to the trade-off synergy degree between WY and SC (34.51%), followed by topography (31.99%), climate (20.92%), and socio-economic factors (11.58%). These results offer valuable insights for decision-makers in

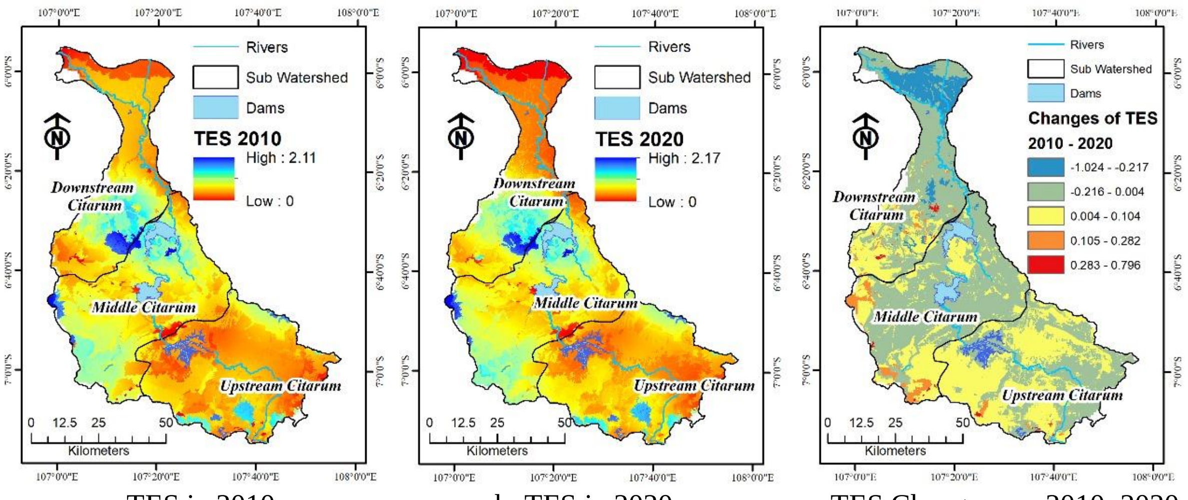

a. TES in 2010 b. TES in 2020 c. TES Change year 2010–2020

Figure 6. Spatial distribution of TES in Citarum Watershed: (a) TES in 2010, (b) TES in 2020, and (c) changes between 2010 and 2020

Table 4. The Citarum Watershed's total amount of TES from 2010 to 2020

Name subwatershed	Area (ha)	TES 2010		TES 2020		Change 2010–2020	
		Mean	Total	Mean	Total	Total	Percent
Upstream	245,413	0.42	1.13	0.42	1.12	-0.01	-0.88
Middle	251,373	0.62	1.72	0.59	1.63	-0.09	-5.23
Downstream	194,130	0.56	1.13	0.46	0.93	-0.20	-17.70
Citarum	690,916	0.53	3.98	0.49	3.68	-0.30	-7.54

designing regional plans and ecological management strategies that promote sustainable development (Nahib et al., 2024b).

Urbanization has brought about social and environmental problems like traffic congestion, social isolation, and rural poverty in this region, and it has also played a major role in land conversion and ES loss (Liu et al., 2019). These results are in line with earlier research, which suggests that LULC is a major factor influencing ES change and that LULC is increasing in both rate and intensity (Lambin and Meyfroidt, 2011). LULC changes in Hubei, China's ES are driven by variations in temperature, rainfall, population density, land use patterns, and socio-economic development levels. Furthermore, prior research has shown that interactions between ES are influenced by climatic conditions and land use types (Sun et al., 2022). Research in the Citarum Watershed found that changes in LULC contributed between 5.8% and 10.42% to variations in WY during the 2000 to 2018 period. In contrast, climate change had a significantly larger impact, contributing between 89.57% and 94.19% (Nahib et al., 2023).

Evaluation of LUC and TES using CCD

A bivariate spatial autocorrelation test used local indicators of spatial association (LISA) to further-investigate the spatial correlation between LUI and TES in Citarum Watershed. The results are shown in Figure 7 and Table 5.

The results of the bivariate spatial autocorrelation test showed that the average values of Moran's I index for TES and LUI in 2010 and 2020 were 0.274 and 0.294 ($p < 0.001$), respectively. These values clarify the spatial correlation between LUI and TES in Citarum Watershed. This implies that LUI and TES have a positive spatial correlation. This means that as LUI increases, TES also increases. The spatial autocorrelation distribution patterns during the research period exhibited consistency between 2010 and 2020, predominantly featuring high-high and low-low patterns. In areas classified as high-high, both the average LUI and average TES were high.

In 2010, 21 sub-districts showed this high-high pattern, which increased to 23 sub-districts in 2020. The middle and downstream areas of Citarum Watershed were characterized by this high-high pattern. Conversely, in areas classified as low-low, both the average LUI and average TES were low, with 24 sub-districts displaying this pattern. This low-low pattern is predominantly found in the upstream areas of Citarum Watershed. In these low-low areas, both the average LUI and TES are low, with 24 sub-districts exhibiting this pattern.

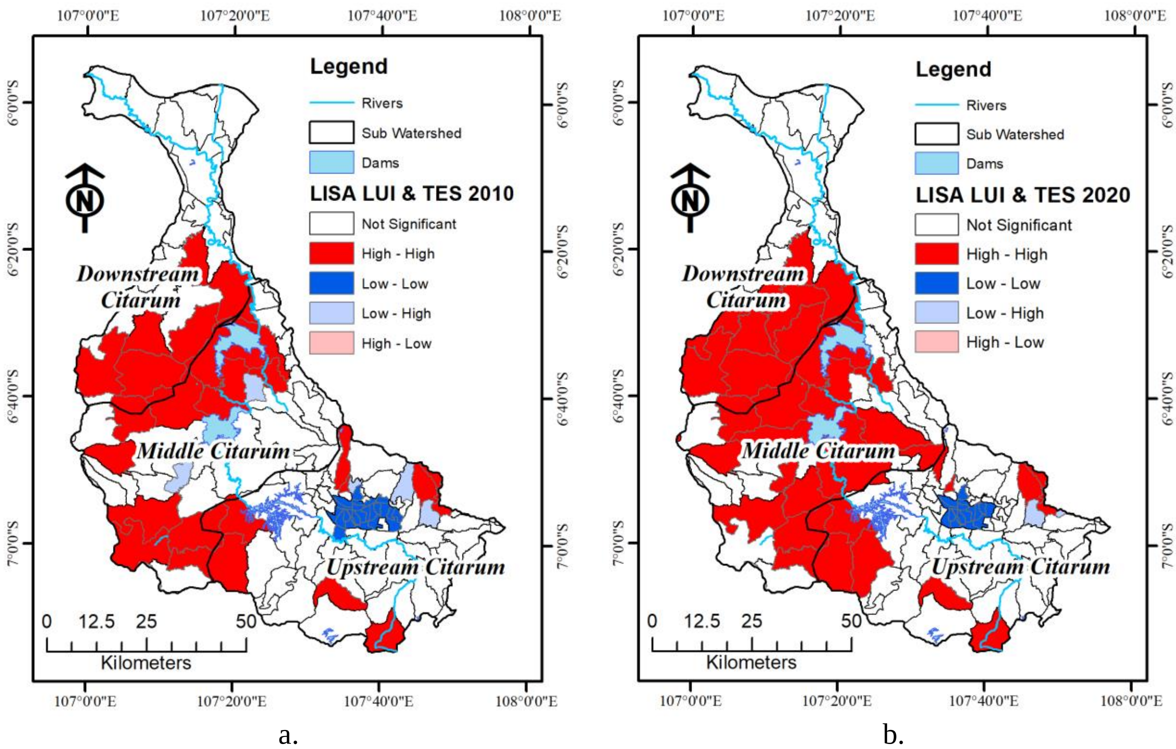

Figure 7. LISA-bivariate cluster maps between LUI and TES from (a) 2010 to (b) 2020

Table 5. LISA-bivariate cluster maps between LUI and TES from 2010 to 2020 on Citarum Watershed (Sub-district scale)

CCD	LISA					
	2010		2020		Change 2010–2020	
	Number*	%	Number*	%	Number *	%
High–High	21	12.88	23	14.11	2	9.52
High–Low	1	0.61	2	1.23	1	100.00
Not significant	109	66.87	107	65.64	-2	(1.83)
Low–Low	24	14.72	24	14.72	0	-
Low–High	8	4.91	7	4.29	-1	(12.50)
Total	163	100.00	163	100.00	-	-

Note: * = Number of sub-districts

CCD for analyzing the interaction between LUI and TES

The spatial distribution of LUI and TES coordination development levels from 2010 to 2020 is presented using the CCD model. The result on the sub-district scale is presented in Table 6 and Figure 8.

Referring to Figure 8 and Table 6, in both 2010 and 2020, the CCD for LUI and TES exhibited the same pattern: the majority of sub-districts (65 to 68%) fell into the imbalance category, while the remaining sub-districts (32 to 35%) were in the balanced category. Regarding temporal changes, the combined CCD for LUI and ES was 0.604 in 2010 and 0.638 in 2020. All coordination levels stayed in the primary coordination state during this time, with 2020 seeing the greatest value and 2010 the lowest, the trend shows an increase. The degree of alignment or mismatch between LUI and TES is reflected in the CCD, which measures the quality of the relationship between humans and land (Liu et al., 2018). Achieving green and sustainable development in China requires accelerating the development of ecological civilization in tandem with economic growth. Sustainable land management techniques and the maintenance of ecosystem functionality in Indonesia depend on an understanding of how LUI affects ES. Studies indicate that improving the amount of vegetation cover, taking part in greening initiatives, and spreading awareness of ecological protection can improve the coordination between LUI and TES. On the other hand, unchecked LULC can impede ES growth and deteriorate this link (He et al., 2022).

During the study period, LUI and TES coordination in Citarum Watershed was usually dominant, with some sub-districts experiencing substantial imbalances. This emphasizes the crucial tension in the human-land relationship, indicating the need for prompt adjustments to land use planning and economic development policies. Overall, the relationship between LUI and TES is complex, with changes in one potentially impacting the other (Wang et al., 2018). In regions such as Indonesia, LUI substantially impacts ES. According to Felipe-Lucia et al. (2020), increased LUI can disrupt ecosystem functioning, diminish biodiversity, and, ultimately, endanger human well-being by interfering with the linkages between biodiversity, ecosystem functions, and services. Their findings also show that higher LUI standardizes synergies between biodiversity, ecosystem functioning, and services. This comprehensive method aids in identifying key ecological features for monitoring and preventing major alterations (Felipe-Lucia et al., 2020).

More detailed studies, such as Liu et al. (2021) on Jiangsu Province, reveal a positive correlation between LUI and regional eco-efficiency. This suggests that appropriate LUI can ensure a continuous supply of eco-products and services from the land ecosystem. The findings show that as LUI increases, the eco-efficiency of Jiangsu Province improves, with a correlation coefficient of 0.683. However, the value of ES provided by the land ecosystem decreases with increased LUI, showing a negative correlation with a coefficient of 0.911. Therefore, reasonable LUI is essential for maintaining the supply of various eco-products and services, thus enhancing regional eco-efficiency. Conversely, extensive and unbalanced land use, without measures to sustain the land ecosystem, can diminish ES and ultimately hinder regional eco-efficiency improvement (Liu et al., 2021).

LUI affects food supply, soil microbial diversity, CS, water conservation, water purification, and habitat quality, among other ES. According to Byers et al. (2024), intensive agricultural techniques can potentially enhance soil carbon loss by broadening the range of microbial genes that break down carbon.

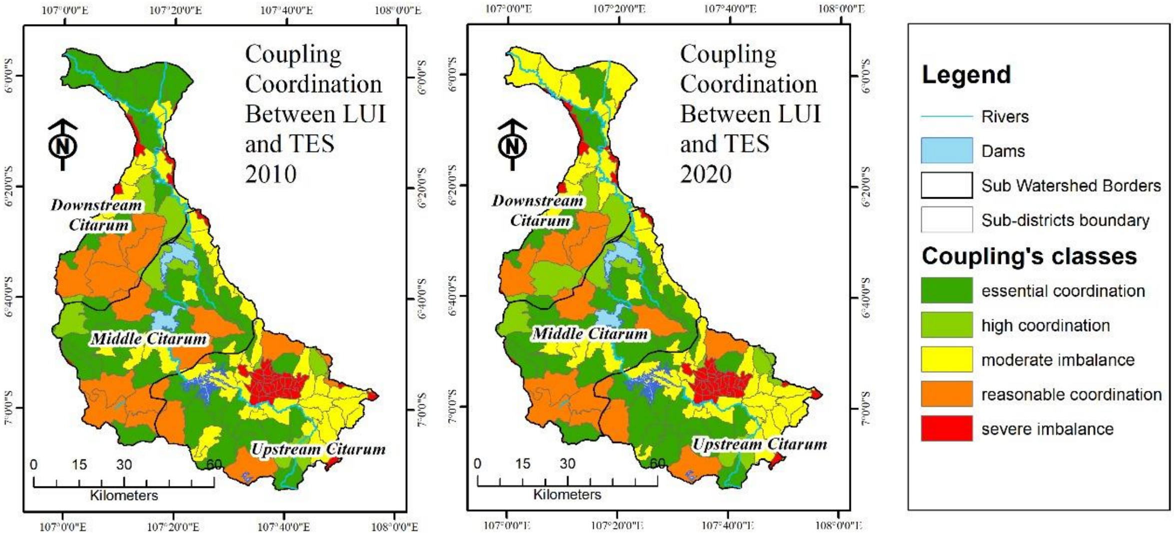

Figure 8. Spatial distribution of coupling coordination between LUI and TES (sub-district scale)

Table 6. CCD between LUI and TES in Citarum Watershed (sub-district scale), 2010 to 2020

CCD	2010		2020		Change 2010–2020	
	N	%	N	%	N	%
Severe imbalance ($0 \leq CCD < 0.2$)	61.00	37.42	62.00	38.04	1.00	1.64
Moderate imbalance ($0.2 \leq CCD < 0.4$)	46.00	28.22	50.00	30.67	4.00	8.70
Necessary coordination ($0.4 \leq CCD < 0.6$)	38.00	23.31	34.00	20.86	-4.00	-10.53
Decent coordination ($0.6 \leq CCD < 0.8$)	15.00	9.20	12.00	7.36	-3.00	-20.00
strong coordination ($0.8 \leq CCD \leq 1$)	3.00	1.84	5.00	3.07	2.00	66.67
Total	163.00	100.00	163.00	100.00	-	-

According to Pereira et al. (2023), LUI also affects ES bundles, exhibiting a negative association with services including CS, water purification, water conservation, and habitat quality, but a favorable correlation with food supply.

Furthermore, intensive agriculture increases greenhouse gas emissions, pollution, soil erosion, biodiversity loss, and greenhouse gas degradation, all of which impact the provisioning, regulation, and cultural aspects of ES (Gomes et al., 2021a). The intensity of land management can change the structure of the food web, favoring longer trophic chains and macropredators, which can affect the stability and functioning of ecosystems. According to Priyadarshini et al. (2019), the conversion of forests into plantation forests (e.g., pine, teak, *Albizia chinensis*, or *Cadamba*) or agricultural areas in the Sumber Brantas Subwatershed, Batu City, East Java, leads to reduced carbon stocks. Effective management practices and the cultivation of woody plants with high biomass are crucial for conserving carbon stocks (Priyadarshini et al., 2019).

Sustainable management in areas with a discrepancy between ES and LUI requires a planned strategy. According to research by Liu et al. (2021), managing trade-offs and regulating ES requires scientific backing. This research highlights the significance of comprehending the spatial characteristics of ES and the influence of human activities on ES supply and demand (Liu et al., 2021). According to Li et al. (2023), their investigation revealed that human activities typically harm several kinds of ES balances, with a few pixels showing a positive influence from the gross domestic product (GDP) the cultivated land ratio, and the area-weighted average patch fractal dimension (Li et al., 2023). The results of Turmudi et al. (2024) study in the Cisadane Watershed, Banten Province, highlight the importance of ES management in achieving sustainable river basin management, particularly amidst the growing demand for natural resources driven by population growth. Furthermore, approximately 50% of sub-districts exhibited unbalanced coordination between LUI and WY in 2010 and 2020.

In contrast, in regions where LUI and ES are well-coordinated, a strategic approach focuses on environmentally friendly urbanization adapted to local conditions. This includes promoting intensive land use in specific areas and establishing ecological pilot zones to protect ecosystems. Studies conducted on Hanjiang River Basin (Yang et al., 2022), Changchun City (Wang et al., 2022), and China's contiguous poor areas (Zhang et al., 2024) emphasize the significance of striking a balance between economic development and environmental preservation. Key strategies include environmental prioritization, sustainable development pathways, and incorporating ES into spatial planning and socio-economic policies.

Integrating prudent LULC into future planning and management is essential to support the beneficial coupling between LULC and TES. Unwise LULC can lead to resource degradation and ecological damage (Bryan et al., 2018). Sustainable LULC development solutions should be used in regions with inadequate coupling coordination to attain both efficient LULC and ecological and environmental benefits. Establishing ecological compensatory systems and putting innovative urbanization plans into practice can help achieve this (Xie et al., 2023). According to Lyu et al. (2022), zoning management that incorporates the characteristics of ES and the socio-ecological environment can effectively identify ecological issues and encourage management recommendations in various socio-ecological contexts. This can provide new perspectives on incorporating ES into actual decision-making and ecosystem management.

In regions with a high CCD, the strategies should focus on promoting balanced development across various subsystems. This can be achieved through several approaches. The first strategy is adopting environmentally sustainable agricultural practices and conservation technologies to reduce water consumption and improve soil health. The second one is implementing regular monitoring and evaluation of CCD to ensure the effectiveness of these strategies (Fan et al., 2023). The third strategy is tailoring policies to local conditions to encourage coordinated and sustainable development (Ge et al., 2023). The last one is raising community awareness about water conservation and sustainable land-use practices.

Efforts to enhance the coordination between LUI and WY include developing an index system to assess urban development intensity and water environmental carrying capacity and evaluating efficiency and interlinkages across various systems, such as high-tech industries (Deng et al., 2023). Additionally, integrating water resource management into land-use planning, as demonstrated in Greece, can play a pivotal role in environmental conservation and sustainable development. This approach emphasizes collaboration between land-use and water management authorities through strategic planning, stakeholder engagement, adaptive management, and continuous monitoring to address water management challenges and protect the environment (Wang and Zhang, 2023).

Limitations of the study and future directions

The objective of this study was to investigate the spatial correlation and connecting characteristics between LUI and ES. One limitation of this study was that spatial interactions between ES and other socio-economic or environmental variables were not considered. Therefore, a potential direction for future investigation is to apply a spatial regression model, namely regionally weighted regression, to delve deeper into the relationship between ES and several impacting variables. Furthermore, the use of advanced methodologies, such as geographic probes, Bayesian spatiotemporal hierarchy models, and other sophisticated approaches, is worth considering to better assess the driving factors. This study focused on the variations in ES driven by changes in land use area without delving into the interconnections among different ES. This gives an additional prospective avenue for future research on ES assessment.

CONCLUSIONS

Between 2010 and 2020, LULC underwent significant changes, with bare/shrubland and agricultural areas expanding by 88.37% and 2.25%, respectively, while forest land and lakes decreased by 0.78% and 0.09%. These LULC changes affected ES values, as total WY and CS declined by 15.01% and 4.98%, whereas SC increased by 12.03%. TES in Citarum Watershed declined by 7.54% from 2010 to 2020, with the most substantial reduction (17.70%) occurring in the downstream region. In 2010, 21 sub-districts exhibited a high-high pattern, which increased to 23 sub-districts by 2020. The coupling coordination between LUI and TES was predominantly imbalanced, with 65 to 68% of sub-districts classified as imbalanced and the remaining 32 to 35% as balanced. These findings highlight the need for more comprehensive management approaches to enhance the balance between LUI and ES, ensuring sustainable development in Citarum Watershed.

ACKNOWLEDGEMENT

This paper is part of a doctoral dissertation research, entitled Spatial Model of Sustainable Watershed Planning Based on Ecosystem Services: A Case Study of Citarum Watershed, West Java Province. The author sincerely thanks: (1) The Directorate of Talent Management, National Research and Innovation Agency, for providing the opportunity to undertake a doctoral program through the degree-by-research scheme (Decree number 111/II/HK/2023 Regarding Participants of the Research-Based Postgraduate Program National Research and Innovation Agency for Year 2023), and (2) the lecturers and staff of the Natural Resources and Environmental Management Science Study Program, Postgraduate School of IPB University, for their invaluable support and guidance in facilitating this research.

REFERENCES

Agaton, M., Setiawan, Y., & Effendi, H. (2016). Land use/land cover change detection in an urban watershed: A case study of upper Citarum Watershed, West Java Province, Indonesia. *Procedia Environmental Sciences*, *33*, 654–660. https://doi.org/10.1016/j.proenv.2016.03.120

Anselin, L. (1988). A test for spatial autocorrelation in seemingly unrelated regressions. *Economics Letters*, *28*(4), 335–341. https://doi.org/10.1016/0165-1765(88)90009-2

Anselin, L. (1995). Local indicators of spatial association—LISA. *Geographical Analysis*, *27*(2), 93–115. https://doi.org/10.1111/j.1538-4632.1995.tb00338.x

Bryan, B. A., Gao, L., Ye, Y., Sun, X., Connor, J. D., Crossman, N. D., ... & Hou, X. (2018). China's response to a national land-system sustainability emergency. *Nature*, *559*(7713), 193–204. https://doi.org/10.1038/s41586-018-0280-2

Byers, A. K., Condron, L., Wakelin, S. A., & Black, A. (2024). Land use intensity is a major driver of soil microbial and carbon cycling across an agricultural landscape. *Soil Biology and Biochemistry, 196*, 109508. https://doi.org/10.1016/j.soilbio.2024.109508

Costanza, R., d'Arge, R., De Groot, R., Farber, S., Grasso, M., Hannon, B., ... & Van Den Belt, M. (1998). The value of the world's ecosystem services and natural capital. *Nature*, *387*(6630), 253–260. https://doi.org/10.1038/387253a0

De Groot, R., Brander, L., Van Der Ploeg, S., Costanza, R., Bernard, F., Braat, L., ... & Van Beukering, P. (2012). Global estimates of the value of ecosystems and their services in monetary units. *Ecosystem Services*, *1*(1), 50–61. https://doi.org/10.1016/j.ecoser.2012.07.005

Deng, H., Yang, J., & Wang, P. (2023). Study on coupling coordination relationship between urban development intensity and water environment carrying capacity of Chengdu–Chongqing economic circle. *Sustainability*, *15*(9), 7111. https://doi.org/10.3390/su15097111

Derdouri, A., Wang, R., Murayama, Y., & Osaragi, T. (2021). Understanding the links between LULC changes and SUHI in cities: Insights from two-decadal studies (2001–2020). *Remote Sensing*, *13*(18), 3654. https://doi.org/10.3390/rs13183654

Development Planning Agency at Sub-National Level of West Java Province. (2008). *Peraturan Daerah Provinsi Jawa Barat Nomor 9 Tahun 2008 Tentang Rencana Pembangunan Jangka Panjang Daerah Provinsi Jawa Barat Tahun 2005-2025*. Retrieved from https://jdih.jabarprov.go.id/page/info/produk/6941

Dong, F., & Li, W. (2021). Research on the coupling coordination degree of "upstream-midstream-downstream" of China's wind power industry chain. *Journal of Cleaner Production, 283,* 124633. https://doi.org/10.1016/j.jclepro.2020.124633

Duraiappah, A. K. (2011). Ecosystem services and human well-being: Do global findings make any sense? *BioScience*, *61*(1), 7–8. https://doi.org/10.1525/bio.2011.61.1.2

Fan, Z., Luo, Q., Yu, H., Liu, J., & Xia, W. (2023). Spatial–temporal evolution of the coupling coordination degree between water and land resources matching and cultivated land use eco-efficiency: A case study of the major grain-producing areas in the middle and lower reaches of the Yangtze River. *Land*, *12*(5), 982. https://doi.org/10.3390/land12050982

Felipe-Lucia, M. R., Soliveres, S., Penone, C., Fischer, M., Ammer, C., Boch, S., ... & Allan, E. (2020). Land-use intensity alters networks between biodiversity, ecosystem functions, and services. *Proceedings of the National Academy of Sciences*, *117*(45), 28140–28149. https://doi.org/10.1073/pnas.2016210117

Fu, B., Zhang, L., Xu, Z., Zhao, Y., Wei, Y., & Skinner, D. (2015). Ecosystem services in changing land use. *Journal of Soils and Sediments*, *15*(4), 833–843. https://doi.org/10.1007/s11368-015-1082-x

Ge, K., Wang, Y., Ke, S., & Lu, X. (2023). Research on the spatiotemporal evolution and driving mechanism of coupling coordinating between green transition of urban land use and urban land use efficiency: A case study of the Yangtze River Delta Region in China. *Environmental Science and Pollution Research*, *31*(46), 57002–57024. https://doi.org/10.1007/s11356-023-31072-9

Gomes, E., Inácio, M., Bogdzevič, K., Kalinauskas, M., Karnauskaitė, D., & Pereira, P. (2021a). Future land-use changes and its impacts on terrestrial ecosystem services: A review. *Science of The Total Environment*, *781*, 146716. https://doi.org/10.1016/j.scitotenv.2021.146716

Gomes, E., Inácio, M., Bogdzevič, K., Kalinauskas, M., Karnauskaitė, D., & Pereira, P. (2021b). Future scenarios impact on land use change and habitat quality in Lithuania. *Environmental Research*, *197*, 111101. https://doi.org/10.1016/j.envres.2021.111101

He, N., Zhou, Y., Wang, L., Li, Q., Zuo, Q., & Liu, J. (2022). Spatiotemporal differentiation and the coupling analysis of ecosystem service value with land use change in Hubei Province, China. *Ecological Indicators*, *145*, 109693. https://doi.org/10.1016/j.ecolind.2022.109693

Husodo, T., Ali, Y., Mardiyah, S. R., Shanida, S. S., Abdoellah, O. S., & Wulandari, I. (2021). Perubahan lahan vegetasi berbasis citra satelit di DAS Citarum, Bandung, Jawa Barat. *Majalah Geografi Indonesia*, *35*(1), 54–63. https://doi.org/10.22146/mgi.61217

Islami, F. A., Tarigan, S. D., Wahjunie, E. D., & Dasanto, B. D. (2022). Accuracy assessment of land use change analysis using Google Earth in Sadar Watershed Mojokerto Regency. *IOP Conference Series: Earth and Environmental Science*, *950*(1), 012091. https://doi.org/10.1088/1755-1315/950/1/012091

Jew, E. K. K., Burdekin, O. J., Dougill, A. J., & Sallu, S. M. (2019). Rapid land use change threatens provisioning ecosystem services in Miombo Woodlands. *Natural Resources Forum*, *43*(1), 56–70. https://doi.org/10.1111/1477-8947.12167

Khairunnisa, F., Tambunan, M. P., & Marko, K. (2020). Estimation of soil erosion by USLE model using GIS technique (A case study of upper Citarum Watershed). *IOP Conference Series: Earth and Environmental Science*, *561*(1), 012038. https://doi.org/10.1088/1755-1315/561/1/012038

Kurniawan, F., Adrianto, L., Bengen, D. G., & Prasetyo, L. B. (2019). The social-ecological status of small islands: An evaluation of island tourism destination management in Indonesia. *Tourism Management Perspectives*, *31*, 136–144. https://doi.org/10.1016/j.tmp.2019.04.004

Lambin, E. F., & Meyfroidt, P. (2011). Global land use change, economic globalization, and the looming land scarcity. *Proceedings of the National Academy of Sciences*, *108*(9), 3465–3472. https://doi.org/10.1073/pnas.1100480108

Li, S.-J., Sheng, M.-J., Li, G., Wang, R., Li, J., Zhang, G.-L., & Xiu, W.-M. (2023). Impacts of land use intensification level on fluvo-aquic cropland soil microbial community abundance and necromass accumulation in North China. *Huan Jing Ke Xue= Huanjing Kexue*, *44*(8), 4611–4622. https://doi.org/10.13227/j.hjkx.202209304

Liu, N., Liu, C., Xia, Y., & Da, B. (2018). Examining the coordination between urbanization and eco-environment using coupling and spatial analyses: A case study in China. *Ecological Indicators*, *93*, 1163–1175. https://doi.org/10.1016/j.ecolind.2018.06.013

Liu, Y., Song, W., & Deng, X. (2019). Understanding the spatiotemporal variation of urban land expansion in oasis cities by integrating remote sensing and multi-dimensional DPSIR-based indicators. *Ecological Indicators*, *96*, 23–37. https://doi.org/10.1016/j.ecolind.2018.01.029

Liu, Y., Sun, H., Shi, L., Wang, H., Xiu, Z., Qiu, X., …, & Wang, C. (2021). Spatial-temporal changes and driving factors of land-use eco-efficiency incorporating ecosystem services in China. *Sustainability*, *13*(2), 728. https://doi.org/10.3390/su13020728

Lyu, R., Clarke, K. C., Tian, X., Zhao, W., Pang, J., & Zhang, J. (2022). Land use zoning management to coordinate the supply–demand imbalance of ecosystem services: A case study in the city belt along the Yellow River in Ningxia, China. *Frontiers in Environmental Science*, *10*, 911190. https://doi.org/10.3389/fenvs.2022.911190

Maimaiti, B., Chen, S., Kasimu, A., Mamat, A., Aierken, N., & Chen, Q. (2022). Coupling and coordination relationships between urban expansion and ecosystem service value in Kashgar City. *Remote Sensing*, *14*(11), 2557. https://doi.org/10.3390/rs14112557

Malik, A. D., Arief, M. C. W., Withaningsih, S., & Parikesit, P. (2023). Modeling regional aboveground carbon stock dynamics affected by land use and land cover changes. *Global Journal of Environmental Science and Management*, *10*(1), 245–266 https://doi.org/10.22034/gjesm.2024.01.16

Malinga, R., Gordon, L. J., Jewitt, G., & Lindborg, R. (2015). Mapping ecosystem services across scales and continents–A review. *Ecosystem Services*, *13*, 57–63. https://doi.org/10.1016/j.ecoser.2015.01.006

Millennium Ecosystem Assessment. (2005). *Ecosystems and human well-being: Wetlands and water synthesis*. Washington, D.C.: World Resources Institute. Retrieved from http://hdl.handle.net/10919/65899

Minister of Public Works and Housing Regulation. (2016). *Citarum river basin water resources management plan 2016*. Retrieved from https://sda.pu.go.id/balai/bbwscitarum/publikasi-perencanaan/rencana-rpsda

Nahib, I., Ambarwulan, W., Sutrisno, D., Darmawan, M., Suwarno, Y., Rahadiati, A., …, & Gaol, Y. L. (2023). Spatial-temporal heterogeneity and driving factors of water yield services in Citarum river basin unit, West Java, Indonesia. *Archives of Environmental Protection*, *49*(1), 3–24. https://doi.org/10.24425/aep.2023.144733

Nahib, I., Amhar, F., Wahyudin, Y., Ambarwulan, W., Suwarno, Y., Suwedi, N., ..., & Ramadhani, F. (2022). Spatial-temporal changes in water supply and demand in the Citarum Watershed, West Java, Indonesia using a geospatial approach. *Sustainability*, *15*(1), 562. https://doi.org/10.3390/su15010562

Nahib, I., Wahyudin, Y., Amhar, F., Ambarwulan, W., Nugroho, N. P., Pranoto, B., …, & Karolinoerita, V. (2024a). Analysis of factors influencing spatial distribution of soil erosion under diverse subwatershed based on geospatial perspective: A case study at Citarum Watershed, West Java, Indonesia. *Scientifica*, *2024*(1), 7251691. https://doi.org/10.1155/2024/7251691

Nahib, I., Widiatmaka, W., Tarigan, S. D., Ambarwulan, W., & Ramadhani, F. (2024b). Exploring ecosystem service trade-offs and synergies for sustainable urban watershed management in Indonesia–A case study of the Citarum River basin, West Java, Indonesia. *Ecological Engineering & Environmental Technology*, *25*(12), 315–332. https://doi.org/10.12912/27197050/195008

Peng, J., Tian, L., Liu, Y., Zhao, M., Hu, Y., & Wu, J. (2017). Ecosystem services response to urbanization in metropolitan areas: Thresholds identification. *Science of the Total Environment*, *607–608*, 706–714. https://doi.org/10.1016/j.scitotenv.2017.06.218

Pereira, P., Bogunovic, I., Inacio, M., Zhao, W., & Barcelo, D. (2023). Agriculture intensification impacts on soil and water ecosystem services. *EGU General Assembly Conference Abstracts* (pp. EGU–1423). https://doi.org/10.5194/egusphere-egu23-1423

Pitaloka, E. F., Karuniasa, M., & Moersidik, S. S. (2020). Time series of forest land cover change in the Upper Citarum Watershed, West Java Province, Indonesia. *E3S Web of Conferences*, *211*, 04001. https://doi.org/10.1051/e3sconf/202021104001

Pranoto, B., Hartulistiyoso, E., Aidi, M. N., Sutrisno, D., Nahib, I., Purwono, N., …, & Rahmila, Y. I. (2024). Assessing the sustainability of small hydropower sites in the Citarum Watershed, Indonesia employing CA-Markov and SWAT models. *Water Supply*, *24*(9), 3253–3268. https://doi.org/10.2166/ws.2024.209

Priyadarshini, R., Hamzah, A., & Widjajani, B. W. (2019). Carbon stock estimates due to land cover changes at Sumber Brantas Sub-Watershed, East Java. *Caraka Tani: Journal of Sustainable Agriculture*, *34*(1), 1–12. https://doi.org/10.20961/carakatani.v34i1.27124

Shao, G., Tang, L., & Liao, J. (2019). Overselling overall map accuracy misinforms about research reliability. *Landscape Ecology*, *34*(11), 2487–2492. https://doi.org/10.1007/s10980-019-00916-6

Sharp, R., Douglass, J., Wolny, S., Arkema, K., Bernhardt, J., Bierbower, W., ... & Wyatt, K. (2020). *InVEST 3.8. 7. User's Guide*. The Natural Capital Project, Standford University, University of Minnesota, The Natural Capital Project. Retrieved from https://naturalcapitalproject.stanford.edu/software/invest

Sholeh, M., Pranoto, P., Budiastuti, S., & Sutarno, S. (2018). Analysis of Citarum River pollution indicator using chemical, physical, and bacteriological methods. *AIP Conference Proceedings*, *2049*(1), 020068. https://doi.org/10.1063/1.5082473

Siswanto, S. Y., & Francés, F. (2019). How land use/land cover changes can affect water, flooding and sedimentation in a tropical watershed: A case study using distributed modeling in the Upper Citarum watershed, Indonesia. *Environmental Earth Sciences*, *78*(17), 550. https://doi.org/10.1007/s12665-019-8561-0

Strassburg, B. B. N., Iribarrem, A., Beyer, H. L., Cordeiro, C. L., Crouzeilles, R., Jakovac, C. C., …, & Visconti, P. (2020). Global priority areas for ecosystem restoration. *Nature*, *586*(7831), 724–729. https://doi.org/10.1038/s41586-020-2784-9

Sun, X., Lu, Z., Li, F., & Crittenden, J. C. (2018). Analyzing spatio-temporal changes and trade-offs to support the supply of multiple ecosystem services in Beijing, China. *Ecological Indicators*, *94*, 117–129. https://doi.org/10.1016/j.ecolind.2018.06.049

Sun, X., Ye, D., Shan, R., Peng, Q., Zhao, Z., & Sun, J. (2022). Effect of physical geographic and socio-economic processes on interactions among ecosystem services based on machine learning. *Journal of Cleaner Production*, *359*, 131976. https://doi.org/10.1016/j.jclepro.2022.131976

Suwardi, S., Darmawan, D., Djajakirana, G., Sumawinata, B., & Al Viandari, N. (2023). Assessing N_2O emissions from tropical crop cultivation in mineral and peatland soils: A review. *Caraka Tani: Journal of Sustainable Agriculture*, *38*(2), 308–326. https://doi.org/10.20961/carakatani.v38i2.75235

Syaban, A. S. N., & Appiah-Opoku, S. (2024). Unveiling the complexities of land use transition in Indonesia's new capital city IKN Nusantara: A multidimensional conflict analysis. *Land*, *13*(5), 606. https://doi.org/10.3390/land13050606

Turmudi, T., Nahib, I., Ambarwulan, W., Suryanta, J., Suwedi, N., Suwarno, Y., …, & Yulianingsani, Y. (2024). Assessment of dynamic water yield using multi scenario of LULC in Cisadane Watershed West Java, Indonesia. *Journal of Infrastructure, Policy and Development*, *8*(15), 9375. https://doi.org/10.24294/jipd9375

Wang, W., Wu, T., Li, Y., Xie, S., Han, B., Zheng, H., & Ouyang, Z. (2020). Urbanization impacts on natural habitat and ecosystem services in the Guangdong-Hong Kong-Macao "Megacity." *Sustainability*, *12*(16), 6675. https://doi.org/10.3390/su12166675

Wang, X., Wang, D., Gao, W., Lu, J., & Jin, X. (2022). Investigation of spatial coupling coordination development: Identifying land system states from the adaptation–conflict perspective. *International Journal of Environmental Research and Public Health*, *20*(1), 373. https://doi.org/10.3390/ijerph20010373

Wang, W., & Zhang, J. (2023). Measuring the coupling coordination of land use functions and influencing factors: A case study in

Beijing. *Frontiers in Ecology and Evolution*, *11*, 1159152. https://doi.org/10.3389/fevo.2023.1159152

Wang, Y., Li, X., Zhang, Q., Li, J., & Zhou, X. (2018). Projections of future land use changes: Multiple scenarios-based impacts analysis on ecosystem services for Wuhan city, China. *Ecological Indicators*, *94*, 430–445. https://doi.org/10.1016/j.ecolind.2018.06.047

Wen, Z., Zheng, H., Smith, J. R., Zhao, H., Liu, L., & Ouyang, Z. (2019). Functional diversity overrides community-weighted mean traits in linking land-use intensity to hydrological ecosystem services. *Science of the Total Environment*, *682*, 583–590. https://doi.org/10.1016/j.scitotenv.2019.05.160

Xiao, R., Lin, M., Fei, X., Li, Y., Zhang, Z., & Meng, Q. (2020). Exploring the interactive coercing relationship between urbanization and ecosystem service value in the Shanghai–Hangzhou Bay Metropolitan Region. *Journal of Cleaner Production*, *253*, 119803. https://doi.org/10.1016/j.jclepro.2019.119803

Xie, Y., Zhu, Q., Bai, H., Luo, P., & Liu, J. (2023). Spatio-temporal evolution and coupled coordination of LUCC and ESV in cities of the Transition Zone, Shenmu City, China. *Remote Sensing*, *15*(12), 3136. https://doi.org/10.3390/rs15123136

Xu, Y., Tang, H., Wang, B., & Chen, J. (2016). Effects of land-use intensity on ecosystem services and human well-being: A case study in Huailai County, China. *Environmental Earth Sciences*, *75*(5), 416. https://doi.org/10.1007/s12665-015-5103-2

Yang, H., Zheng, L., Wang, Y., Li, J., Zhang, B., & Bi, Y. (2022). Quantifying the relationship between land use intensity and ecosystem services' value in the Hanjiang River Basin: A case study of the Hubei Section. *International Journal of Environmental Research and Public Health*, *19*(17), 10950. https://doi.org/10.3390/ijerph191710950

Yulianto, F., Nugroho, G., Aruba Chulafak, G., & Suwarsono, S. (2021). Improvement in the accuracy of the postclassification of land use and land cover using landsat 8 data based on the majority of segment-based filtering approach. *The Scientific World Journal*, *2021*(1), 6658818. https://doi.org/10.1155/2021/6658818

Yusuf, S. M., Murtilaksono, K., Hidayat, Y., & Suharnoto, Y. (2018). Analysis and prediction of land cover change in upstream Citarum Watershed. *Jurnal Pengelolaan Sumberdaya Alam dan Lingkungan (Journal of Natural Resources and Environmental Management)*, *8*(3), 365–375. https://doi.org/10.29244/jpsl.8.3.365-375

Zhang, H., Wang, Y., Wang, C., Yang, J., & Yang, S. (2022). Coupling analysis of environment and economy based on the changes of ecosystem service value. *Ecological Indicators*, *144*, 109524. https://doi.org/10.1016/j.ecolind.2022.109524

Zhang, J., Lu, X., Qin, Y., Zhang, Y., & Yang, D. (2024). Can urbanization-driven land-use and land-cover change reduce ecosystem services? A case of coupling coordination relationship for contiguous poverty areas in China. *Land*, *13*(1), 82. https://doi.org/10.3390/land13010082

Zhang, Z., & Li, Y. (2020). Coupling coordination and spatiotemporal dynamic evolution between urbanization and geological hazards–A case study from China. *Science of the Total Environment*, *728*, 138825. https://doi.org/10.1016/j.scitotenv.2020.138825

Zheng, H., Peng, J., Qiu, S., Xu, Z., Zhou, F., Xia, P., & Adalibieke, W. (2022). Distinguishing the impacts of land use change in intensity and type on ecosystem services trade-offs. *Journal of Environmental Management*, *316*, 115206. https://doi.org/10.1016/j.jenvman.2022.115206

Zhu, S., Huang, J., & Zhao, Y. (2022). Coupling coordination analysis of ecosystem services and urban development of resource-based cities: A case study of Tangshan City. *Ecological Indicators*, *136*, 108706. https://doi.org/10.1016/j.ecolind.2022.108706

Appendix 1. The dataset, processing a source for ES

Parameter/Data	Description	Data and value	Source
Precipitation (mm)	Map of average annual precipitation	Annual average rainfall (mm) Raster	Published on Nahib et al. (2022)
Rainfall and temperature	The National Bureau of Meteorology, Climatology, and Geophysics; Citarum Ciliwung River Basin Center; PT. Jasa Tirta II	Numerical/Table data, with location coordinates; a spline interpolation technique	Raster data with a spatial resolution of 30 m
Reference evapotranspiration (mm)	The amount of water that vaporizes from land into the air over a given period. It is the sum of evaporation (directly off of soil, bodies of water, and other surfaces) and transpiration (through plants)	Global potential average evapotranspiration (mm) Raster	Terra Modis Yearly L4 Global (https://earthexplorer.usgs.gov/)
Soil	Soil depth is the soil depth (mm)	A comprehensive soil characteristics dataset	(http://globalchange.bnu.edu.cn/research/soil2)
Soil erodibility map (K factor)	Indonesian Soil Research Institute (The soil map type of 1:100,000)	Vector file	30 m x 30 m
Soil type data: Soil texture, organic matter content, and effective rooting depth	Citarum Ciliwung River Basin Center	Extraction and resampling, conversion from polygon to raster	Raster data with a spatial resolution of 30 m
LULC maps 2010	Landsat/8 OLI imageries with acquisition date in 2010 (https:/www.usgs.gov/ and Google Earth Engine)	Supervised classification	30 m x 30 m
LULC maps 2020	US Geological Survey, http://www.usgs.govUSGS path/row122-121/64	Supervised classification	Raster data with a spatial resolution of 30 m
Boundary shapefile (watershed)	Map of watershed boundaries	Integer (ws_id) from one to n. Vector file (.shp)	College of Forestry, Environment and Resources Management; Ministry of environment and forestry, Republic of Indonesia
Data biophysical table (P USLE and C USLE)	FAO.org	CSV File (Values assigned per land use/land cover (.csv)	30 m x 30 m

Appendix 2. Data of land use intensity and TES based on zonal statistical tools on the ArcGIS 10.8

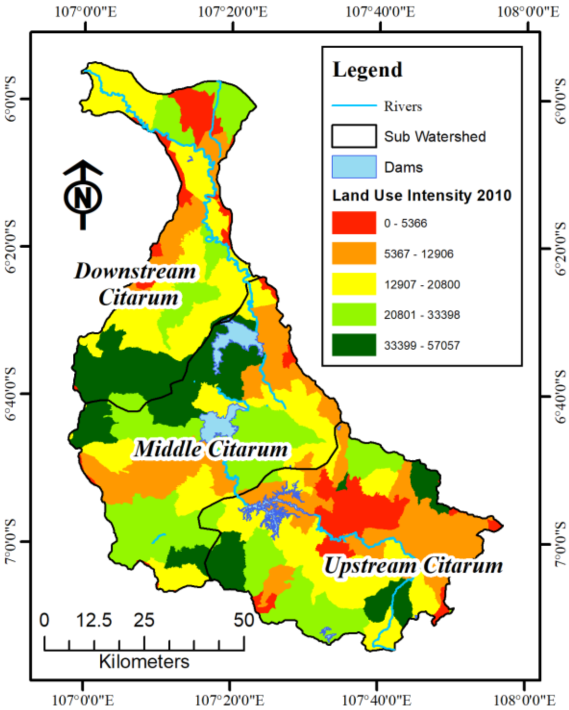

(a) Land Use Intensity 2010

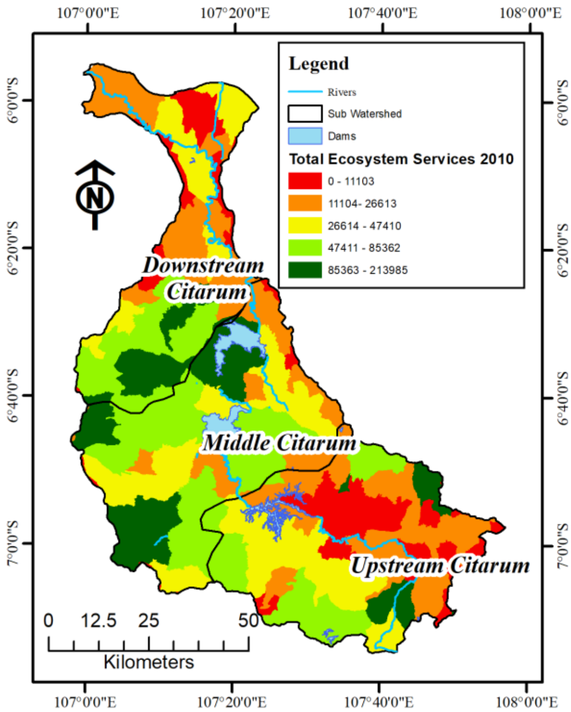

(b) Total Ecosystem Services 2010

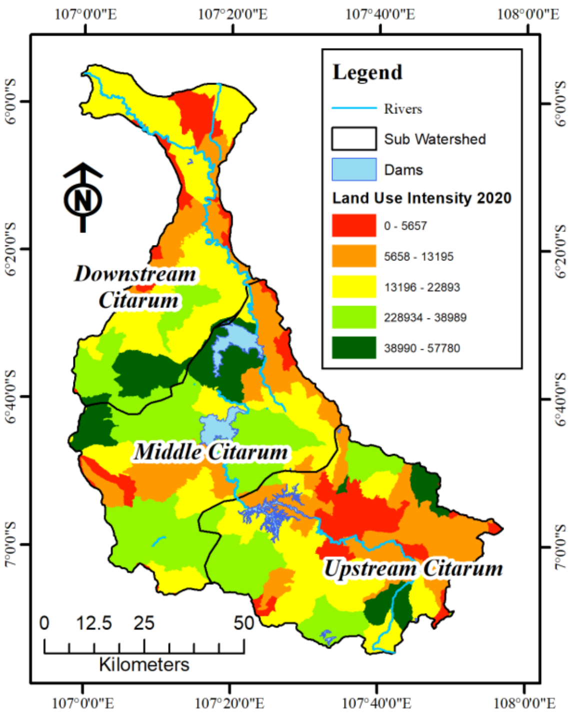

(c) Land Use Intensity 2020

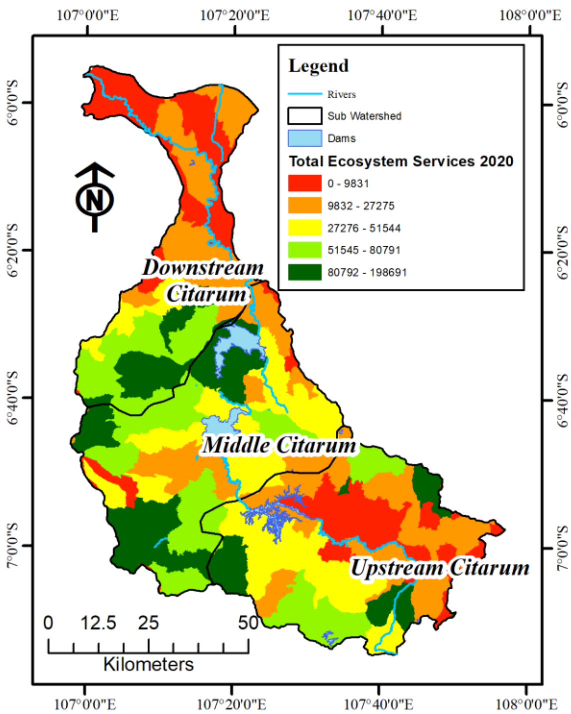

(d) Total Ecosystem Services 2020